Available online at www.sciencedirect.com

SciVerse ScienceDirect

Scripta Materialia 66 (2012) 203–206

Scripta MATERIALIA

www.elsevier.com/locate/scriptamat

A grain boundary phase transition in Si–Au

Shuailei Ma,[a] Kaveh Meshinchi Asl,[b] Chookiat Tansarawiput,[c] Patrick R. Cantwell,[a] Minghao Qi,[c] Martin P. Harmer[a,*] and Jian Luo[b,*]

[a] *Department of Materials Science and Engineering, Center for Advanced Materials and Nanotechnology, Lehigh University, Bethlehem, PA 18015, USA*

[b] *School of Materials Science and Engineering, Center for Optical Materials Science and Engineering Technology, Clemson University, Clemson, SC 20634, USA*

[c] *School of Electrical and Computer Engineering, Birck Nanotechnology Center, Purdue University, West Lafayette, IN 47907, USA*

Received 20 September 2011; accepted 7 October 2011
Available online 14 October 2011

A grain boundary transition from a bilayer to an intrinsic (nominally clean) boundary is observed in Si–Au. An atomically abrupt transition between the two complexions (grain boundary stabilized phases) implies the occurrence of a first-order interfacial phase transition associated with a discontinuity in the interfacial excess. This observation supports a grain-boundary complexion theory with broad applications. This transition is atypical in that the monolayer complexion is absent. A model is proposed to explain the bilayer stabilization and the origin of this complexion transition.

Keywords: Grain boundary; Phase transition; Complexion; Interfaces; Aberration-corrected STEM

Phase transitions are of great importance for understanding and controlling materials fabrication and resultant properties. While they normally occur between bulk phases, materials physicists have long recognized the existence and importance of surface phase transitions, most notably premelting [1] and prewetting [2] transitions. Cahn [3] recognized that grain boundaries (GBs) can also undergo phase transitions. A series of more recent studies suggest that premelting/prewetting like interfacial transitions can occur at GBs [4–13]. Notably, six generic conformations of GB phases, namely, an intrinsic/clean GB, a Langmuir–McLean type monolayer (submonolayer), a bilayer, a trilayer, a nanoscale intergranular film of an equilibrium thickness and a complete wetting film of an arbitrary thickness, have been identified and named as complexions [4,5,14–21]; the formation of these generic GB complexion types can be interpreted from the interplay of GB premelting, prewetting and multilayer adsorption [5,8]. The recognition of GB phase behaviors and the identification of the non-classical complexion types has provided new insights towards the understanding of several outstanding scientific problems in materials science regarding the origins of abnormal grain growth [4,14], solid-state activated sintering [22–24] and liquid metal embrittlement [25].

If the observed GB complexion types can be treated as interfacial phases, one would expect the occurrence of interfacial phase transitions, which can be either continuous or first-order (abrupt). Indeed, thermodynamic models support the existence of such GB transitions [4,5,7,8,12,21]. Recognizing and controlling such GB transitions is of practical importance because they can cause abrupt changes in microstructural development and properties [4,14,15,21]. While an analogous first-order surface transition was revealed recently [26,27], experimental evidence for the occurrence of GB transitions at internal interfaces is sparse. A recent study made a single observation of the co-existence of a bilayer and a (presumably metastable) trilayer at the same GB in Ni–Bi [25], implying the existence of a GB transition between them. In the present study, we demonstrate unequivocally the occurrence of a bilayer to intrinsic/clean GB transition in Si–Au, and we further show that this interfacial transition is likely a first-order one. This observed interfacial transition is unique in that this bilayer to clean GB transition occurs in the absence of

* Corresponding authors. E-mail addresses: mph2@lehigh.edu; jluo@alum.mit.edu

1359-6462/$ - see front matter © 2011 Acta Materialia Inc. Published by Elsevier Ltd. All rights reserved.
doi:10.1016/j.scriptamat.2011.10.011

a monolayer. A model is proposed to explain the bilayer stabilization in this system and the physical origin of the observed first-order complexion transition.

The Si bicrystal specimens (with a 100 nm thick Au film sandwiched between two Si crystals) were made using (1 1 1) float zone wafers. The purchased wafers were cut, cleaned ultrasonically in acetone for 5 min, immersed in a piranha solution ($2H_2SO_4$:$1H_2O_2$) for 10 min, treated by a standard procedure to remove organic contaminates in a solution of $1NH_4OH$:$1H_2O_2$:$1.5H_2O$ at 80 °C for 10 min, dipped in 1% HF for 2 min (to remove surface native oxide), rinsed with deionized water and dried using an N_2 stream. The wafers were then immediately placed in the vacuum chamber and coated with a ~50 nm thick Au film. The bicrystals were made by aligning and bonding the Au-coated wafers with ~15° misorientation to produce a low-symmetry Σ 43 GB. The specimens were annealed using a MHI vertical furnace in the presence of flowing gas (Ar–5% H_2), and Ti sponges were used as getters. The annealing temperature was nominally 1 K below the melting temperature of Si ($T^{Si}_{melting} = 1683$ K); i.e. if we increased the set temperature by 1 K, the silicon wafers would melt (the temperature was monitored by a second thermocouple placed near the specimen, and the monitored temperature fluctuation was about ±1 K). After isothermal annealing of 5 h, the specimens were pulled out of the furnace heating zone into a cold zone flowing forming gas. The temperature (as monitored by the thermocouple near the specimen) was reduced from the nominal annealing temperature of 1682 K to 1000 K in ~1.5 min, then from 1000 K to 600 K in an additional ~3 min. The specimens were then cut transversely, ground with silicon carbide papers up to 1200 grit, polished with 1.0 and 0.3 μm alumina suspensions, and cleaned in acetone. A Hitachi SU6600 scanning electron microscope was used to observe the cross-sections preliminarily. Transmission electron microscopy (TEM) specimens were prepared by using a combination of a focused ion beam instrument (FEI Strata DB 235) and a careful low-energy ion milling technique (Fischione 1010), and characterized using an aberration-corrected scanning transmission electron microscope (JEOL 2200FS) equipped with an energy-dispersive X-ray spectroscopy (EDXS) detector. Micrographs reported here are Z-contrast high-angle annular dark-field (HAADF) images.

Figure 1(a) shows the tip of a withdrawing Au-based drop formed during cooling (a solidified Au particle in the cooled specimen). Several regions of the GB segments were observed, as shown in Figure 1(b)–(d). Note that this particular GB is a (1 1 1) 15° twist GB (Σ 43). In Region B, which is immediately adjacent to the Au particle (Fig. 1(b)), an Au-based bilayer is observed. This continuous bilayer is more than 100 nm long, with uniform thickness; we scanned over the entire length and found that the bilayer exhibited similar character in HAADF scanning TEM (STEM) imaging. In Region D, which is sufficiently far away from the Au particle (Fig. 1(d)), a clean GB, which is essentially free of observable Au adsorption in the HAADF STEM micrograph, is observed. In between, Region C is composed of small segments of bilayers and clean GB segments. The bilayer segment shown in Figure 1(c) is only 5–6 nm wide in the projected direction when the GB is edge-on. It is important to note that a series of careful tilting experiments confirmed that the observed Au bilayer did not form from a projection of steps. Presumably, the wetting and adsorption configurations shown in Figure 1 formed during specimen cooling. A future study is needed to determine whether these 5–6 nm wide discontinuous Au bilayers in Region C (Fig. 1(c)) are islands or strips (nanobelts) in three dimensions, as this is beyond the scope of this work. To support the major conclusion of the current study (as elaborated subsequently), it is important to emphasize that the 5–6 nm wide discontinuous bilayers in Region C also transition sharply to clean GB segments at both ends.

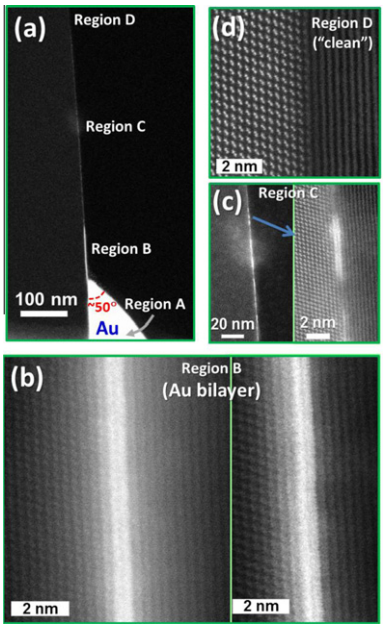

Figure 1. HAADF STEM micrographs of (a) a withdrawing Au drop at the interface of a Si bicrystal, which presumably formed during cooling. (b–d) Views of Regions B, C and D, respectively, at higher magnifications.

In Z-contrast HAADF STEM micrographs, the bilayers are characterized by their bright contrast by virtue of the high Z number of Au. EDX analyses directly confirmed the enrichment of Au in the bilayer. Moreover, the bright contrast of the bilayers in HAADF STEM micrographs appears to extend significantly and diffusely into both adjacent grains. EDXS analysis of a point that is 5 nm away from the bilayer (inside the adjacent grain) also revealed the presence of a small amount of Au. Although it is difficult to exclude beam spreading effects, the combination of HAADF STEM imaging and EDXS analyses suggests that some Au is "dissolved" in both grains to form a nanoscale diffuse Au segregation/adsorption profile. The maximum bulk solid solubility of Au in Si is $\sim 1.5 \times 10^{17}$ atoms cm^{-3}, or ~30 ppm (atomic fraction), occurring at ~1300 °C. However, the "solubility" in the first few atomic layers near the GB core can certainly be much higher than the bulk solubility, as demonstrated elegantly in a model developed by Wynblatt and Chatain (even if their specific model and formulae were derived for face-centered cubic metals) [28].

A careful analysis of the HAADF STEM images shows that the Au layer in each of the bilayers is adsorbed coherently on the adjacent Si grain. In STEM images, it is difficult to resolve the periodic structures in both Si grains and Au bilayers simultaneously because of the significantly different brightness (as a consequence of a large difference in the Z numbers). Figure 2 displays the same HAADF STEM image at two different contrast and brightness levels to correlate the periodic structures in the Si grains with the associated Au bilayer. This pair of images demonstrates the coherence between the atom positions in one of the Si grains and its adjacent Au layer (one layer in the bilayer). Since this is a symmetrical twist GB, the two grains are crystallographically equivalent to each other with mirror plus rotation operations and therefore the Au atoms in the other layer are also coherently adsorbed on its adjacent grain. Although it is not possible to resolve the periodic structures in both Au layers simultaneously due to the 15° twist, we were able to confirm this coherent Au adsorption by tilting each Si crystal to the appropriate zone axis. Since this is a low-symmetry (Σ 43) GB and each Au layer in the bilayer is adsorbed coherently onto the adjacent Si grain, there must be a large mismatch between the two adsorbed Au layers in the bilayer (i.e. a lattice match following only the Σ 43 periodicity). The proposed atomistic configuration for the bilayer is schematically illustrated in Figure 3(b).

Perhaps the most striking observation of this study is the coexistence of bilayers and clean/intrinsic GB segments at the same GB, as vividly shown in Figure 3(a), an image obtained at the boundary between Regions C and D. This indicates the occurrence of a bilayer to clean GB transition, which presumably took place during cooling. Furthermore, the atomically abrupt transitions between the two GB complexions (Fig. 4(a) as well as Fig. 1(c)) suggests that the GB structural and chemical (phase) transition from a bilayer to an intrinsic/clean GB is likely a first-order one, because it is associated with a discontinuity (i.e. an abrupt "jump") in the interfacial excess of the solute (Au) adsorption.

Surprisingly, our observations showed that bilayers transition to intrinsic/clean GBs in the absence of the intermediate state (complexion) of monolayers (Figs. 1(c) and 3(a)). Figure 3(b) schematically illustrates the relative stabilities of a bilayer, a monolayer and an intrinsic/clean GB, as well as the origin of the first-order bilayer to intrinsic GB transition; here we adopted a

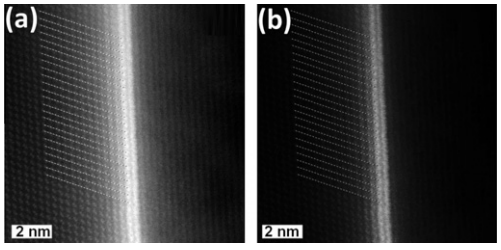

Figure 2. A HAADF STEM micrograph displayed at the two different brightness levels. The set of parallel lines plotted at the same locations indicates coherence between one of the adsorbed Au layer and its adjacent Si grain.

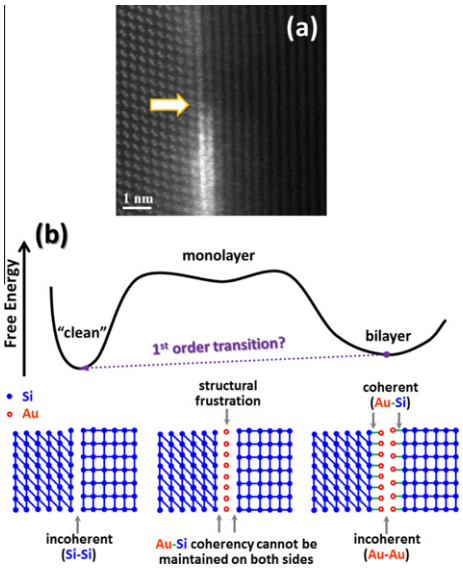

Figure 3. (a) HAADF STEM micrograph showing the abrupt transition region between the bilayer and the "clean" GB, indicating the occurrence of a first-order GB phase transition between them. (b) Schematic illustration of bimodal free-energy states that may lead to a first-order transition, the origin of which can be explained from the negative mixing enthalpy of the Au–Si system (indicating that it is energetically favorable to form Au–Si bonds from breaking Au–Au and Si–Si bonds); see text for elaboration.

simplified regular-solution lattice-gas model, following a similar model that was recently proposed to explain the stabilization of bilayers in Ni–Bi (see Fig. S11 in Ref. [25]). Like the Ni–Bi case, a bilayer in Si–Au can be stabilized if Au atoms bond strongly to the Si atoms on the adjacent Si grain surface. To test this assumption, we used the Miedema model [29] and free software developed by Dr. R.F. Zhang [30] to estimate the formation enthalpy for an $Au_{0.5}Si_{0.5}$ alloy and found it to be -7.997 kJ mol^{-1} (i.e. Au–Si bonds are energetically favored to form from breaking Si–Si and Au–Au bonds). As illustrated in Figure 3(b), it may be energetically more expensive to form an Au monolayer at the low-symmetry (Σ 43) twist GB because the Au monolayer cannot grow coherently with respect to both grain surfaces; i.e. some strong Au–Si bonds must be broken at (at least) one Si–Au interface. In other words, the monolayer complexion may represent a high energy state because the tendency of both Si grain surfaces would be to impose structural order onto the monolayer and this structural ordering is incompatible (because this is a low-symmetry Σ 43 GB); this may result in a structural frustration that destabilizes the monolayer complexion. In contrast, in a bilayer, each Au layer can follow the order of their adjacent grain, resulting in the breaking of the Au–Au bonds between the two adsorbed layers, which are likely weaker than Si–Au bonds because of the negative regular solution parameter; thus this bilayer complexion can be energetically more stable in the present case.

Schulli et al. [31] reported "substrate-enhanced supercooling" in the Au–Si system, in which they used in situ X-ray scattering to demonstrate the "interface-enhanced stabilization" of nanometer-thick, Au-based, liquid-like films on the Si (1 1 1) surface to ~120 K below the eutectic

temperature and ~360 K below the liquidus line. Prior high-resolution TEM characterization of quenched specimens has directly shown the stabilization of nanoscale, impurity-based, liquid-like (amorphous-like) films on free surfaces [27,32–35] and at GBs [6,24,36] in ceramic materials. Similar nanoscale equilibrium-thickness intergranular films (one of the six Dillon–Harmer complexion types [4,5,14–21]) have also been found at metallic GBs [9–11,23] and oxide–metal interfaces [37–41]. Considering that Au–Si is a metallic glass forming system, one would expect nanoscale "amorphous" films to be a stable complexion at a twist (1 1 1) GB (where the crystallization would be even more difficult than the case of a liquid-like Au film on a Si (1 1 1) surface in the prior report [31]). Somewhat surprisingly, this study showed the stabilization of a much more ordered complexion, namely bilayers. The bilayer interfacial phase (Dillon–Harmer Complexion III) has been observed previously in both ceramic [4,16,17] and metallic [25] systems.

The occurrence of GB structural transitions was suggested by a prior atomistic simulation conducted for twist (1 0 0) GBs in pure Si [42]. Direct comparison of the current experimental results of a twist (1 1 1) GB in the Si–Au binary system and the prior modeling results of twist (1 0 0) GBs in pure Si [42] are not justified. Nonetheless, the current study provides the most convincing evidence for the existence of GB structural (phase) transitions; such evidence was sparse in the prior literature, thereby making the current observation valuable.

In summary, we have observed a GB-stabilized phase (complexion) transition from a bilayer to an intrinsic/clean GB in Si–Au and have shown that this GB phase transition is likely a first-order one. A model is proposed to explain the stabilization of the bilayer complexion and the origin of this first-order bilayer to intrinsic GB transition in the absence of an intermediate state of a monolayer. In general, the occurrence of GB transitions can often lead to abrupt changes and/or abnormal behaviors in materials fabrication (e.g. enhanced sintering [22–24]), microstructural evolution (e.g. abnormal grain growth [4,14]) and materials properties (e.g. embrittlement [25]). This observation supports a new GB complexion theory, which recognizes GB phase behavior, uses it to solve a wide range of mysteries in materials science and helps to realize predictable fabrication of materials by design [4,14,15,21,22,25].

The authors would like to thank Prof. Steve Pennycook in Oak Ridge National Laboratory for helpful discussion. We gratefully acknowledge the financial support from the U.S. DOE Office of Basic Energy Science Grants in the Electron and Scanning Probe Microscopies Program: Grant No. DE-FG02-08ER46511 for J.L. K.M.A, M.Q. and C.T., and Grant No. DE-FG02-08ER46548 for M.P.H. and S.M., both managed by Dr. Jane G. Zhu.

[1] J.G. Dash, A.M. Rempel, J.S. Wettlaufer, Rev. Mod. Phys. 78 (2006) 695.
[2] J.W. Cahn, J. Chem. Phys. 66 (1977) 3667.
[3] J.W. Cahn, J. Phys. Paris 43 (1982) C6.
[4] S.J. Dillon, M. Tang, W.C. Carter, M.P. Harmer, Acta Mater. 55 (2007) 6208.
[5] M. Tang, W.C. Carter, R.M. Cannon, Phys. Rev. Lett. 97 (2006) 075502.
[6] J. Luo, Crit. Rev. Solid State Mater. Sci. 32 (2007) 67.
[7] Y. Mishin, W.J. Boettinger, J.A. Warren, G.B. McFadden, Acta Mater. 57 (2009) 3771.
[8] J. Luo, Appl. Phys. Lett. 95 (2009) 071911.
[9] J. Luo, V.K. Gupta, D.H. Yoon, H.M. Meyer, Appl. Phys. Lett. 87 (2005) 231902.
[10] X. Shi, J. Luo, Appl. Phys. Lett. 94 (2009) 251908.
[11] X. Shi, J. Luo, Phys. Rev. Lett. 105 (2010) 236102.
[12] J. Mellenthin, A. Karma, M. Plapp, Phys. Rev. B 78 (2008) 184110.
[13] S. Divinski, M. Lohmann, C. Herzig, B. Straumal, B. Baretzky, W. Gust, Phys. Rev. B 71 (2005) 104104.
[14] M.P. Harmer, J. Am. Ceram. Soc. 93 (2010) 301.
[15] M.P. Harmer, Science 332 (2011) 182.
[16] S.J. Dillon, M.P. Harmer, Acta Mater. 55 (2007) 5247.
[17] S.J. Dillon, M.P. Harmer, J. European Ceram. Soc. 28 (2008) 1485.
[18] S.J. Dillon, M.P. Harmer, J. Am. Ceram. Soc. 91 (2008) 2304.
[19] S.J. Dillon, M.P. Harmer, G.S. Rohrer, Acta Mater. 58 (2010) 5097.
[20] S.J. Dillon, M.P. Harmer, G.S. Rohrer, J. Am. Ceram. Soc. 93 (2010) 1802.
[21] S.J. Dillon, M.P. Harmer, J. Luo, JOM 61 (12) (2009) 38.
[22] J. Luo, Curr. Opin. Solid State Mater. Sci. 12 (2008) 81.
[23] V.K. Gupta, D.H. Yoon, H.M. Meyer III, J. Luo, Acta Mater. 55 (2007) 3131.
[24] J. Luo, H. Wang, Y.-M. Chiang, J. Am. Ceram. Soc. 82 (1999) 916.
[25] J. Luo, H. Cheng, K. Meshinchi Asl, C.J. Kiely, M.P. Harmer, Science 333 (6050) (2011) 1730. doi: 10.1126/science.1208774.
[26] H. Qian, J. Luo, Acta Mater. 56 (2008) 4702.
[27] H.J. Qian, J. Luo, Appl. Phys. Lett. 91 (2007) 061909.
[28] P. Wynblatt, D. Chatain, Metall. Mater. Trans. A 37A (2006) 2595.
[29] F.R. de Boer, R. Boom, W.C.M. Mattens, A.R. Miedema, A.K. Niessen, Cohesion in Metals: Transition Metals Alloys, North-Holland, Amsterdam, 1988.
[30] R.F. Zhang, Miedema Calculator (Ver. 2.1; available at http://www.zrftum.wordpress.com/), 2011.
[31] T.U. Schulli, R. Daudin, G. Renaud, A. Vaysset, O. Geaymond, A. Pasturel, Nature 464 (2010) 1174.
[32] J. Luo, Y.-M. Chiang, Annu. Rev. Mater. Res. 38 (2008) 227.
[33] J. Luo, Y.-M. Chiang, R.M. Cannon, Langmuir 21 (2005) 7358.
[34] J. Luo, Y.-M. Chiang, Acta Mater. 48 (2000) 4501.
[35] J. Luo, Y.-M. Chiang, J. European Ceram. Soc. 19 (1999) 697.
[36] H. Wang, Y.-M. Chiang, J. Am. Ceram. Soc. 81 (1998) 89.
[37] M. Baram, D. Chatain, W.D. Kaplan, Science 332 (2011) 206.
[38] M. Baram, W.D. Kaplan, J. Mater. Sci. 41 (2006) 7775.
[39] A. Avishai, C. Scheu, W.D. Kaplan, Z. Metallkd. 94 (2003) 272.
[40] A. Avishai, C. Scheu, W.D. Kaplan, Acta Mater. 53 (2005) 1559.
[41] C. Scheu, G. Dehm, W.D. Kaplan, J. Am. Ceram. Soc. 84 (2001) 623.
[42] S. von Alfthan, K. Kaski, A.P. Sutton, Phys. Rev. B 76 (2007) 245317.